

# Use of Direct-Modulated/Gain-Switched Optical Links in Monopulse-Type Active Phased Array Systems

Siou Teck Chew, *Student Member, IEEE*, Dennis Tak Kit Tong, Ming C. Wu, *Member, IEEE*, and Tatsuo Itoh, *Fellow, IEEE*

**Abstract**—With the advance of high speed laser technology, optical interaction with microwave circuits has become highly viable. Such interaction is advantageous as the fiber is low-loss, lightweight, and immune to electromagnetic interference. In this paper, interaction of direct-modulated and gain-switched optical links with active antenna phased array systems is demonstrated. In the direct-modulated optical system, the RF signal directly modulates the DFB laser. In the gain-switched optical system, the laser is gain-switched to function as a RF frequency doubler. The modulated signal is transmitted via an optical fiber and recovered at the receiving end by a high-speed photodetector. The recovered RF is then injected into the active antenna phased array systems as an injection-locking reference signal. Two active antenna systems are used for this demonstration: beam-switching and Doppler transceiver.

## I. INTRODUCTION

THERE HAS BEEN extensive research in the interaction of optical signals with microwave circuits. As direct modulation bandwidth is constantly being pushed higher in the development of high speed lasers, optical interaction with RF circuits becomes viable. Currently, state-of-art high speed laser diodes have a direct modulation bandwidth of 30 GHz [1]. This makes direct modulation of a laser diode an easy and efficient method for RF-optical signal conversion.

Use of optical link is very attractive and viable, as the fiber is low loss, highly deformable, lightweight, and immune to electromagnetic interference. This is favorable for radar systems where space and weight are critical constraints. In addition, optical fiber has the capability of simultaneous multiple-wavelength transmission and reception in wavelength-multiplexing communication system. Modeling and analysis of this optical/RF link have been extensively studied and reported [2]–[4]. However, the microwave systems used are conventional in nature.

A new system design approach in the area of microwave front-ends is to make use of the active antenna concept. In this approach, RF circuit functions are transferred to the antenna platform. High density integration of these circuits is

Manuscript received January 10, 1995; revised November 12, 1995. This work was supported in part by US Army Research Office Contract DAAH04-93-G-0068 and by the Joint Services Electronics Program F49620-92-C-0055 and ARPA NCIPT.

The authors are with the Department of Electrical Engineering, University of California, Los Angeles, CA 90095 USA.

Publisher Item Identifier S 0018-9480(96)01455-X

made possible by appropriate planar or multi-layered structures. Thus, patch antennas can be integrated with microwave circuits on one substrate. The advantage of this approach is that transmitted RF power generation is distributed to each element of the antenna. This means that the system does not require complex and bulky waveguide structures for power combining/dividing. Furthermore, RF signal processing like frequency conversion can also be distributed to each element of the active antenna. Thus, the RF signal suffers less loss and may require less amplification. To date, active antenna system designs include not only power combining [5]–[6], but also beam-scanning [7]–[8].

Optical interaction has been demonstrated for single microstrip patch antennas [9]. Recently, application of an optical link in an active phased array for beam-scanning has been reported [10]. The optical interaction serves as a link and is passive in nature. However, this link can play an active role by providing some form of control functions, like adjusting phase delay [11], to the microwave system.

In this paper, an attempt is made to demonstrate optical interaction with the active antenna systems, specifically the monopulse-type phased arrays. Both direct-modulated and gain-switched optical links will be implemented. In the direct-modulated link, a  $2 \times 2$  phased array capable of beam-switching in both azimuth and elevation planes is used. The optical link carries a 6.6 GHz reference signal for injection-locking of the active antenna. In the gain-switched optical link, the nonlinearity of a gain-switched laser has been exploited as a frequency doubler. This is particularly attractive at millimeter wave frequencies as stable signal sources are difficult to implement and direct modulation of a millimeter wave signal to a laser is not trivial. As a proof of concept, an active  $2 \times 1$  Doppler transceiver operating at 6.5 GHz is used with a stable reference signal for injection-locking pumped into the optical link at 3.25 GHz.

## II. DESIGN

### A. System Configuration

The conceptual system shown in Fig. 1 is used. The system consists of four subcircuits: 1) a laser diode to convert RF to an intensity-modulated optical signal, 2) a length of fiber to carry the modulated lightwave to the active antenna, 3) a high speed

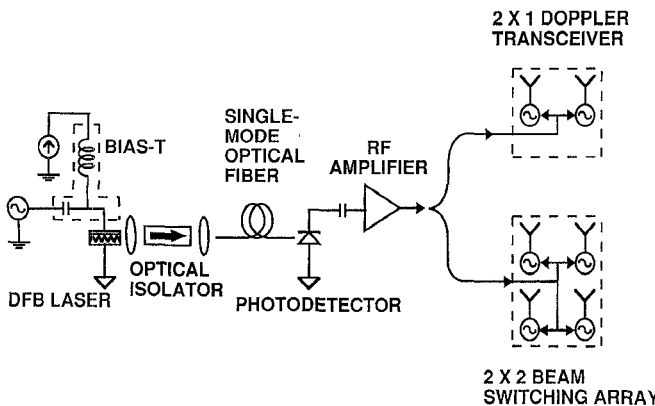


Fig. 1. Schematic diagram of the system setup.

photodetector/amplifier subcircuit to recover the RF signal from the optical signal, and 4) the active antenna arrays, which are fed by the recovered RF signal for injection locking.

### B. Phase Control in Active Antenna

For the active antenna designs in this paper, injection-locking is used to create the desired phase relationships among the antenna elements. Based on Kurokawa's theory [12], the phase difference between a free-running signal and an injected signal is related by

$$\Delta\phi = \sin^{-1} \left( \frac{\omega_f - \omega_0}{2\Delta\omega_m} \right) \quad (1)$$

where  $\omega_f$  is the free-running frequency,  $\omega_0$  is the injected signal frequency and  $2\Delta\omega_m$  is the locking bandwidth. From (1), a phase difference of  $\pm 90^\circ$  is possible by varying either the injection frequency or the free-running frequency. With an increase in injected power,  $2\Delta\omega_m$  also increases.

In the active antennas used here, the phase difference is not varied continuously. Instead, the circuit switches between three phase difference states, namely  $\Delta\phi = +90^\circ, -90^\circ$ , and  $0^\circ$ . This is achieved by tuning the free-running frequency of the oscillators.

### C. Direct-Modulated System

**Optical Circuit:** In this setup, the RF-to-optical conversion is achieved by direct modulating a distributed feedback (DFB) laser. A DFB laser is preferred over the Fabry-Perot laser because it has better relative intensity noise (RIN) and hence better signal-to-noise ratio performance [13]. By superimposing the RF reference signal on the laser drive current, the light intensity can be modulated accordingly. Here, an InGaAsP-InP DFB laser, operating at  $1.31 \mu\text{m}$ , is used. It is mounted on a coplanar waveguide which is impedance-matched to the  $50 \Omega$  coaxial components. The threshold current and external quantum efficiency are 24 mA and 250 mW/A, respectively.

It is noted that the 3 dB modulation bandwidth increases with the dc biasing current until the laser saturates at large biasing current. For the laser used here, the 3 dB modulation bandwidth is 16 GHz when biased at 60 mA. To convert the RF signal to an optical signal, the DFB laser is prebiased such that

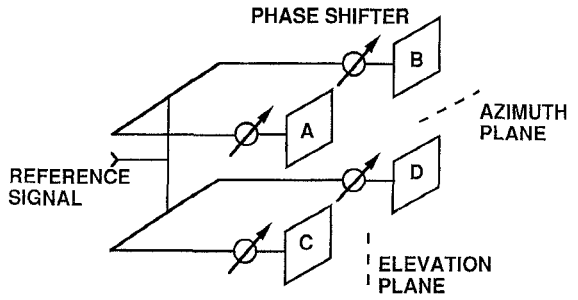


Fig. 2. Schematic diagram of a phased antenna array.

the frequency response peaks at the RF operating frequency of 6.6 GHz. The RF reference signal is then superimposed on the biasing current through a bias tee. The modulated lightwave is coupled by lenses into a three-meter long single mode fiber. An optical isolator is inserted between lenses to minimize reflections between them. At the receiving end, a high speed photodetector (HP 83 440D) with a bandwidth of 34 GHz is used to detect and reconvert the optical signal into RF signal.

When biased at 30 mA, the measured link efficiency is  $-32.9$  dB at 6.6 GHz. This efficiency can be accounted for by the following expression [14]

$$G = 10 * \log \left( \frac{\rho_{LB} \eta_{LB}^2 t_{od}^2 \eta_D^2 R_D \rho_D}{R_L} \right) \quad (2)$$

where  $R_L$  is the equivalent resistance of the laser diode above threshold,  $R_D$  is the photodiode's equivalent resistance,  $\eta_{LB}$  is the laser diodes slope efficiency,  $\eta_D$  is the photodiode's slope efficiency,  $t_{od}$  is the fiber's optical transfer efficiency,  $\rho_{LB}$  is the matching circuit loss of the laser diode, and  $\rho_D$  is the matching circuit loss of the photodiode. From (2), the major sources of the link loss are fiber coupling and laser diode's conversion efficiency. Slight impedance mismatch at both ends of the link also introduce some loss. The RIN of the laser is less than  $-125$  dB/Hz, which corresponds to a link noise figure better than 57 dB [14].

Amplifiers are used in the setup to increase the power level to a sufficient level for injection locking before pumping the signal into the active antenna system.

**Beam-Switching Active Phased Array:** In this system, the array is designed with the capability of switching the antenna beam bidirectionally between sum and difference patterns in both the azimuth and elevation planes. Based on the  $2 \times 2$  phase array in Fig. 2, the desired phase relationships to synthesize the respective patterns are tabulated in Table I.

The schematic diagram of the beam-switching array is shown in Fig. 3. The patch antenna serves both as a resonator as well as a radiator. The upper and lower quadrants are fed on the opposite sides of the patch antenna, resulting in  $180^\circ$  excitation. This layout is desirable as space is a constraint. Also, when the free-running frequencies of the oscillators are tuned to the reference frequency, a difference pattern is formed in the elevation plane. This means the phase relationship is stable, as compared to the free-running frequency tuned to the band-edge [15]. However, this desired arrangement is not possible for the azimuth plane due to layout constraints. Thus,

TABLE I  
PHASE RELATIONSHIPS AMONG ANTENNAS FOR BEAM-SWITCHING

PHASE CONDITIONS	AZIMUTH PLANE	ELEVATION PLANE
$A=B=C=D=0^\circ$	SUM	SUM
$A=B=90^\circ, C=D=-90^\circ$	SUM	DIFFERENCE
$A=C=90^\circ, B=D=-90^\circ$	DIFFERENCE	SUM

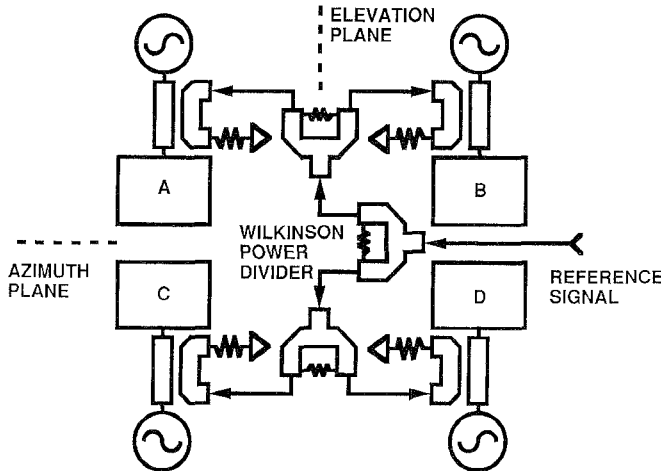


Fig. 3. Schematic diagram of the beam-switching array.

the phase relationship must be offset accordingly from that in Table I. Wilkinson power dividers are used to distribute the injected signal to each oscillator.

This circuit is fabricated on substrate with  $\epsilon_r = 2.33$  and thickness 30 mils. The isolation between the two output ports of the Wilkinson power divider is about 18 dB. The oscillators are designed using NEC72084 FET's, self-biased at  $I_{ds} = 30$  mA with  $V_{ds} = 3$  V, operating at 6.6 GHz. The frequency is tuned via the drain bias and the tuning range is at least 40 MHz. The locking range is about 20 MHz. The antenna elements are spaced  $0.7\lambda_0$  at 6.6 GHz.

#### D. Gain-Switching System

**Optical Circuit:** In this setup, the gain-switched laser diode functions as a RF-to-optical converter as well as a RF frequency doubler. A multiquantum well InGaAs-InGaAsP distributed feedback (DFB) laser, operating at  $1.55 \mu\text{m}$  is used for gain-switching. The threshold current and external quantum efficiency of the DFB laser are 15 mA and 36 mA/W respectively. An SMA connector is in direct contact with the laser. Gain-switching is achieved by biasing it just above threshold and modulating its gain by a 3.25 GHz RF signal. The output of the gain-switched laser, in the time domain, is a train of optical pulses with a repetition rate of 3.25 GHz and an estimated pulse width of 30 ps. Its frequency spectrum consists of a fundamental signal at 3.25 GHz and a series of higher order harmonics. The modulated optical signal is transmitted through a single mode optical fiber. At the receiver's end, a high speed photodetector is used for optical-to-RF conversion.

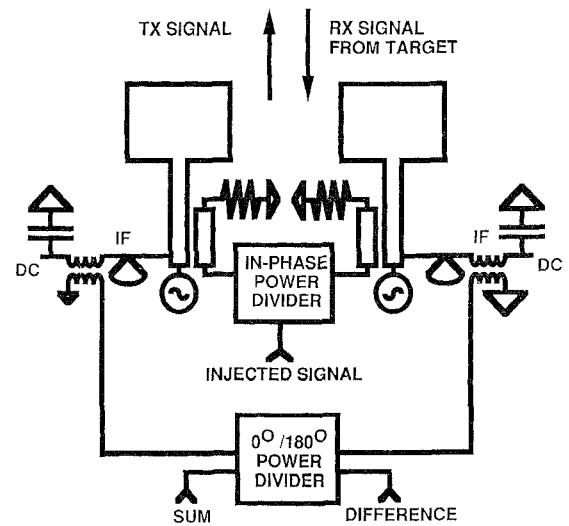


Fig. 4. Schematic diagram of the Doppler transceiver array

The second harmonic component at 6.5 GHz is extracted with a RF filter, and then amplified for injection locking. The optical link conversion efficiency, which we define here as the ratio of the average power of the second harmonic component at 6.5 GHz detected by the photodetector to the average power of the modulating signal at 3.25 GHz, is approximately  $-48$  dB. This conversion efficiency can be improved with better optical coupling and impedance matching to the coaxial components. Full quantitative analysis of the link efficiency and noise figure requires further investigation.

**Doppler Transceiver:** The microwave subsystem is a  $2 \times 1$  active antenna array, as shown in Fig. 4. The phased array functions as a transceiver. The transmitter generates RF power quasi-optically. When the transmitted signal is reflected from a moving target, a Doppler shifted signal is returned. When received by the phased array, a self-oscillating mixer is used to produce an IF output signal at the Doppler frequency.

The patch antenna is used as the radiating element as well as the resonator for the oscillator element. The NEC72084 FET is used as the active device in the oscillator/mixer design. The MESFET is biased at  $V_{ds} = 3$  V and  $I_{ds} = 30$  mA. This bias condition is used for higher oscillating signal power and not for optimum mixing condition. Thus, the mixer performance has been compromised.

To ensure effective quasi-optical power combination at broadside, the oscillating signal of each element in the array must be in-phase. In-phase oscillation of each element also allows the phase relationship among the RF signals of the array

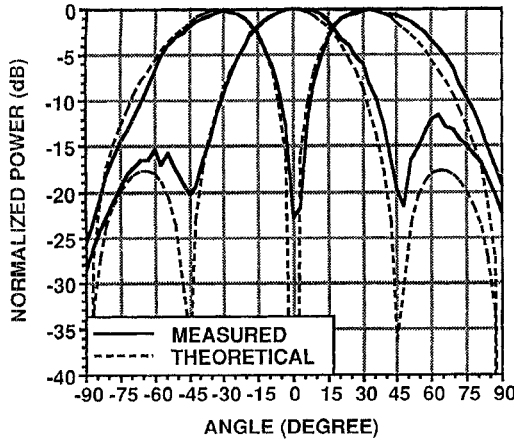


Fig. 5. Measured and calculated sum and difference patterns in the azimuth plane of the beam-switching array.

to be maintained in the IF. This synchronization is achieved through injection-locking. To reduce circuit complexity, only one antenna is used at the drain of the MESFET to allow higher power to be transmitted. Since the RF signal is pumped into the drain the conversion loss is expected to be lower than that pumped into the gate of the MESFET. The IF signal is tapped through a transformer at the drain bias circuit.

To provide direction tracking, the monopulse concept is used at IF by using a  $0^\circ/180^\circ$  planar drop-in power divider to generate the sum and difference channels. When both IF signals from each antenna element are fed into the E and H ports of the power divider simultaneously, the sum and difference channels are synthesized. Both channels are then amplified externally. With both sum and difference signals, an error voltage can be generated which is used for tracking.

### III. RESULTS

The measured sum and difference patterns of the beam-switching array in the azimuth plane are shown in Fig. 5. The measured patterns agree well with that calculated from a simple transmission-line model. There is a difference in the power level of the peaks in the difference pattern. This is because when the oscillators are tuned to different free-running frequencies for the desired phase relationship, the locked output signal power of each oscillator is different. Another reason is that as frequency tuning is achieved through drain bias, there is a variation of RF power. The measured patterns in the elevation plane of the beam-switching array are shown in Fig. 6. Both patterns suffer slight distortion, due to radiation from the rest of the circuit. This can be eliminated by using a multi-layered structure. Also, possible mutual coupling among the elements can create the distortion.

In general, when operating at the frequency band-edge, stability is an issue. One way to resolve this problem is to allow the circuit not to operate at the band-edge and additional phase shift is used either with delay lines or active phase shifters.

As for the Doppler transceiver, the measured oscillation frequency is 6.5 GHz. Fig. 7 shows the measured transmit antenna pattern. The sum and difference channels are then measured with a signal radiating at broadside to simulate the

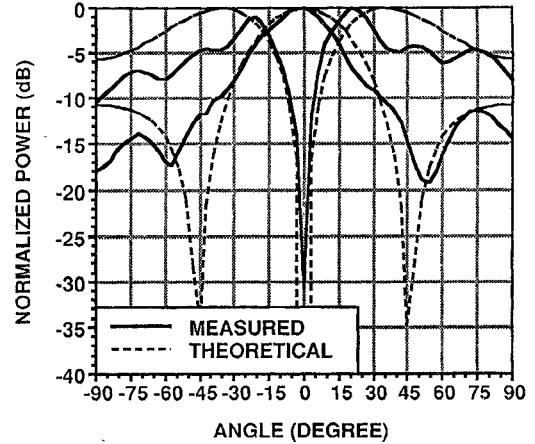


Fig. 6. Measured and calculated sum and difference patterns in the elevation plane of the beam-switching array.

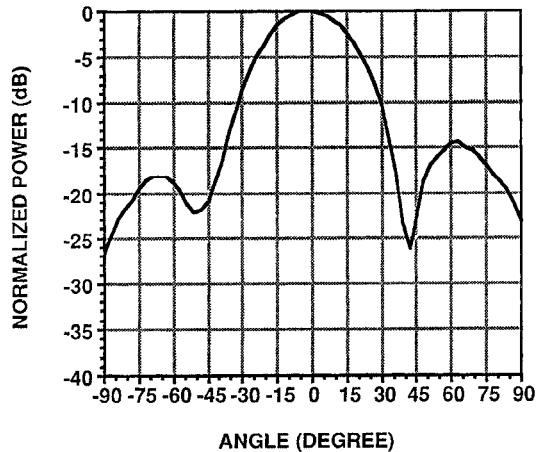


Fig. 7. Measured transmit pattern of the Doppler transceiver array.

Doppler frequency shift. A Doppler frequency shift of 5 MHz is used here to test the system as the  $0^\circ/180^\circ$  power divider has a lower band-edge frequency of 5 MHz. It is recognized that the Doppler frequency shift is much lower than 5 MHz. The power divider is chosen out of availability and does not affect the principle of operation. The measured receiver patterns of the sum and difference channels are shown in Fig. 8. As the radiated power is concentrated within  $\pm 45^\circ$ , only data within that range are presented. There is a slight asymmetry in all the measured patterns. This is due to poor asymmetric mixer performance and phase imbalance in the injection-locking and the  $0^\circ/180^\circ$  power divider. This can be corrected by introducing active phase shifters into the circuit for fine tuning.

### IV. CONCLUSION

In this paper, integration of an optical subsystem with RF monopulse-type active antenna phased arrays has been demonstrated. An optical reference signal has been transmitted via a fiber link to the RF active antenna arrays. Both direct-modulated and gain-switched optical links are implemented with beam-switching and Doppler transceiver antenna arrays respectively. The gain-switched optical link functions as a

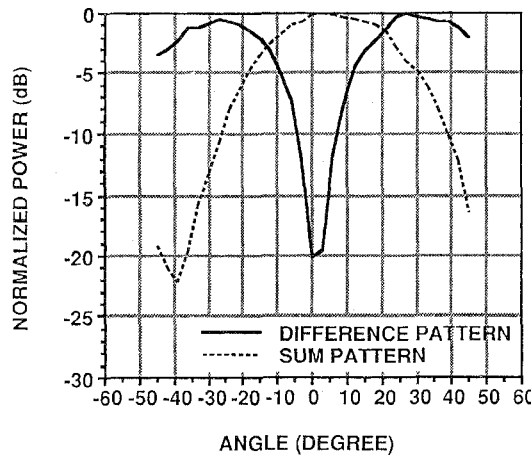


Fig. 8. Measured sum/difference pattern of the Doppler transceiver array at IF.

frequency doubler in the system. For higher frequency applications, e.g., 94 GHz, the higher harmonics of a monolithic mode-locked laser can be used instead. Indeed, with the use of optical link, the system noise figure is higher compared with that of a microwave link. Also, due to the link loss, larger amplification is required to boost the recovered RF to a level sufficient for injection locking.

#### REFERENCES

- [1] S. D. Offsey, L. F. Lester, W. J. Schaff, and L. F. Eastman, "High-speed modulation of strained-layer InGaAs-GaAs-AlGaAs ridge waveguide multiple quantum well lasers," *Appl. Phys. Lett.*, vol. 58, pp. 2336-2338, May 1991.
- [2] X. Zhou and A. S. Daryoush, "An efficient self-oscillating mixer for communications," *IEEE Trans. Microwave Theory Tech.*, vol. 42, no. 10, pp. 1858-1862, Oct. 1994.
- [3] A. S. Daryoush, E. Ackerman, N. R. Samant, S. Wanuga, and D. Kasemset, "Interfaces for high-speed fiber-optic links: Analysis and experiment," *IEEE Trans. Microwave Theory Tech.*, vol. 39, pp. 2031-2044, Dec. 1991.
- [4] C. H. Cox III, G. E. Betts, and L. M. Johnson, "An analytic and experimental comparison of direct and external modulation in analog fiber-optic links," *IEEE Trans. Microwave Theory Tech.*, vol. 38, pp. 501-509, May 1990.
- [5] K. D. Stephan, "Inter-injection-locked oscillators for power combining and phased arrays," *IEEE Trans. Microwave Theory Tech.*, vol. MTT-34, pp. 1017-1025, Oct. 1986.
- [6] J. Birkeland and T. Itoh, "Spatial power combining using push-pull FET oscillators with microstrip patch resonators," in *IEEE MTT-S Int. Microwave Symp. Dig.*, 1990, vol. 3, pp. 1217-1220.
- [7] J. Lin, S. T. Chew and T. Itoh, "A unilateral injection-locking type active phased array for beam-scanning," *IEEE MTT-S Int. Microwave Symp. Dig.*, 1994, vol. 2, pp. 1231-1234.
- [8] P. Liao and R. A. York, "Phase-shifterless beam-scanning using coupled-oscillators: Theory and experiment," in *IEEE AP-S Int. Symp. Dig.*, 1993, vol. 2, pp. 668-671.
- [9] A. J. Svitak, D. M. Pozar, and R. W. Jackson, "Optically fed aperture-coupled microstrip patch antennas," *IEEE Trans. Antennas Propagat.*, vol. 40, pp. 85-90, Jan. 1992.
- [10] S. T. Chew, T. K. Tong, M. C. Wu, and T. Itoh, "An active phased array with optical input and beam-scanning capability," *IEEE Microwave Guided Wave Lett.*, vol. 4, no. 10, pp. 347-349, Oct. 1994.
- [11] W. Ng, A. A. Walston, G. L. Tangonan, J. J. Lee, I. L. Newberg, and N. Berstein, "The first demonstration of an optically steered microwave phased array antenna using true-time-delay," *J. Lightwave Technol.*, vol. 9, pp. 1124-1131, 1991.
- [12] K. Kurokawa, "Injection locking of microwave solid-state oscillators," in *Proc. IEEE*, Oct. 1973, vol. 61, pp. 1386-1410.
- [13] K. Y. Lau, C. M. Gee, T. R. Chen, N. Bar-Chaim, and I. Urym, "Signal-induced noise in fiber-optic links using directly-modulated fabry-perot and distributed-feedback laser diodes," *J. Lightwave Technol.*, vol. 11, pp. 1216-1225, 1993.
- [14] R. Simons, *Optical Control of Microwave Devices*. Boston: Artech House, 1990.
- [15] P. S. Hall, I. L. Morrow, P. M. Haskins, and J. S. Dahele, "Phase control in injection locked microstrip active antenna," in *IEEE MTT-S Dig.*, 1994, vol. 2, pp. 1227-1230.

**Siou Teck Chew, (S'94)** for a photograph and biography, see this issue, p. 274.



**Dennis Tak Kit Tong** received the B.S. degree from the University of Maryland, College Park, in 1993, and the M.S. degree from the University of California, Los Angeles, in 1995, both in electrical engineering. His master thesis involved high-speed direct-detected and coherent optical fiber links. He is currently working toward the Ph.D. degree at the University of California, Los Angeles.

His research interests include optically controlled phased array antenna, high-speed optical fiber link and wavelength-division-multiplexed laser source.



**Ming C. Wu** (S'80-M'88) received the M.S. and Ph.D. degrees in electrical engineering from the University of California, Berkeley, in 1985 and 1988, respectively.

From 1988 to 1992, he was a Member of Technical Staff in the Semiconductor Electronics Research Department of AT&T Bell Laboratories, Murray Hill, NJ, where he conducted research in ultrafast semiconductor integrated optoelectronics, high speed semiconductor lasers, and monolithic mode-locked semiconductor lasers. In 1993, he joined the faculty of Electrical Engineering Department of UCLA as Associate Professor. His current research interests include ultrafast integrated optoelectronics, ultrafast high power photodetectors, semiconductor lasers, optical interconnect, micro-opto-mechanical systems, optical MEMS and their applications, free-space integrated optics. He served as the General Co-Chair of the IEEE LEOS Summer Topical Meeting on RF Optoelectronics in 1995, and will serve as the General Co-Chair of the Topical Meeting on Optical MEMS and Their Applications in 1996, and in Program Committee of CLEO 1996. He has more than 70 journal papers and 80 refereed conference presentations, and holds 6 U.S. patents.

Dr. Wu is a member of IEEE OSA, APS URSI, Eta Kappa Nu, and a Packard Foundation Fellow.

**Tatsuo Itoh, (S'69-M'69-SM'74-F'82)** for a photograph and biography, see this issue p. 274.